T1. High current H^- ion source development at RRCAT

V.K. Senecha (senecha@rrcat.gov.in) and Ajeet Kumar

High-energy and high-current circular accelerators of the new generation favour H^- ions since they offer the possibility to use charge exchange multi-turn injection into the synchrotron ring with high conversion efficiency to protons [1]. They eliminate the problems associated with extreme ramping required for injection kickers encountered with positive-ion facilities and higher beam losses leading to higher radioactivity and activation of components of ring accelerator. Further, in the International Thermonuclear Energy Reactor (ITER), it acts as an efficient tool for heating fusion plasma through higher energy neutral atoms for applications with high neutralization efficiency [2].

At Raja Ramanna Centre for Advanced Technology, we have initiated the task to develop a high current H^- ion source delivering ion beam having 50 keV energy, 35 mA current, 0.5 ms pulse duration and 25 Hz repetition rate. This ion source would serve as a crucial component of 3 MeV front-end H^- injector Linear accelerator (Linac), being developed as a part of ongoing XI plan project. At 100 MeV linac energy, the beam can be injected in the rapid cycling synchrotron (RCS) which will accelerate and deliver 1GeV proton beam for the ultimate goal of establishing pulsed spallation neutron source (SNS).

H^- ions can be produced using a hybrid scheme based on both surface[3] as well as volume production[4] processes giving higher yield. The hydrogen gas plasma can either be produced through an arc discharge using a filament (W/LaB_6) or else a RF coil antenna. However, the hydrogen plasma essentially needs to be confined using multi-cusp magnetic field configuration surrounding the plasma chamber. The cusp field can be created by using an array of NdFeB permanent magnets (PM's) of field strength ~ 0.25 T, mounted all around the cylindrical plasma chamber with alternating polarity. In order to design such magnetic field configuration, we have performed computer simulations using finite element analysis for cylindrical geometry. The simulation results have been verified by experimental field measurements according to which, the radial magnetic field variation inside an aluminium cylinder having 12 NdFeB PM's, show a power law functional form rather than the exponential form considered by many workers[5]. We have carried out the physics design studies pertaining to two types of H^- ion sources- (i) A filament based arc discharge driven multi-cusp ion source [6] and (ii) RF antenna discharge driven multi-cusp ion source[7,8]. In order to optimize the ion beam properties, one has to perform the computer simulation using some standard ion extraction code that can simulate the beam extraction considering the effect of space charge and sheath formation near the extraction region. One can optimize the extraction geometry considering appropriate shape, size and inter-separation of two, three, four or five electrode geometry. This can lead to desired beam parameters required for linac system.

In this article, we present the basic physics of H^- ion formation and destruction processes followed with the computer simulations of H^- ion source to do the physics design studies and verification of some of the simulation results through experiments.

I. Production of H^- ions:

a. Surface generation:

In the surface process, the negative ion production is realized on the electrodes, in contact with the gas discharge plasma. The H atoms and H_n^+ ions (n=1,2,3) would be converted into H^- ions on collision with a low work function electrode. For this reason the electrodes of special emitters with a very low work function (with Cesium (Cs) mono-layer deposition reducing the work-function φ of W or Mo metals to < 2eV) is used for the enhancement of negative ion production. The H^- ions are produced on a surface in two ways (i) Hydrogen atoms (H) hit the wall having low work-function and are bounced back as H^- ions. This process is called atomic process and can be of two types. In first type, the high energy H atom interacts with the wall and bounce back as H^- ion. For this process the energy of the H atom must be above the work function of the surface. The yield depends on the Cs coverage of the surfaces. In the second type, when low energy H atom is adsorbed on the wall surface and captures one electron from the surface and subsequently evaporated as an H^- ion from the wall and goes back to the plasma. This mechanism is known as "surface ionization". Surface ionization is possible only if the electron affinity of the surface is smaller than that of H atom, which is 2.1 eV. In such case, this process is energetically convenient to generate an H^- ion, even in the case of zero kinetic energy of the H atom. (ii) The hydrogenic ions (H^+, H_2^+, H_3^+) hit the wall and are emitted as H^- ions from a surface covered with low work-function metal like Cs or Ba. This process is called ionic process. Here the sheath formation in the plasma chamber plays a crucial role as the positive ions are accelerated in the sheath near the wall by the sheath potential. If the energy of those accelerated ions is of the order of ~20 eV, the H^- ion yield is near the maximum for a Cs/Mo surface having work function 1.7 eV. In cases where H^+ is reflected from the surface, this energy is roughly equal to the particles incident energy, typically determined by the plasma sheath potential through which particles striking the surface must fall.

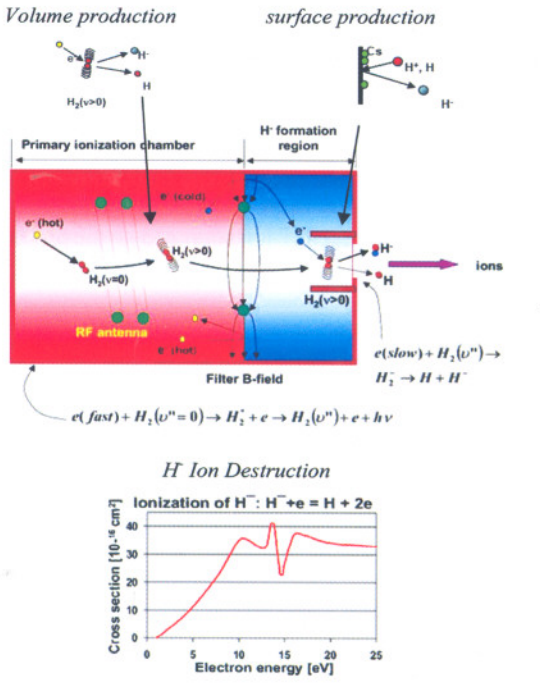

Fig. T.1.1 Schematic of RF based ion source depicting the volume and surface production of H⁻ ions and their destruction cross-section variation with energy

b. Volume generation:

In the volume process, the H^- ions are formed directly in the plasma volume through two-step electron-neutral collisional processes [9-10]. These processes are:

1) Creation of high concentration of vibrationally and rotationally excited H_2^* (v") molecular state. Here (v") denotes the vibrational state.

$$e(fast) + H_2(v''=0) \rightarrow H_2^* + e \rightarrow H_2(v'') + e$$

2) H_2 (v") molecules dissosiatively attach (DA) with low energy electrons ~ 1eV and make H^- ions.

$$e(slow) + H_2(v'') \rightarrow H_2^* \rightarrow H^- + H$$

It has been shown that the cross section for dissociative attachment reaction can be increased by more than five orders of magnitude if H_2 is in a heightened state of vibrational excitation. The cross sections for H^- formation achieve a maximum of ~10^{-16} cm^2 colliding with excited H_2 (v">5) at relative energies of ~1 eV. One of the most important excitation mechanisms is electron impact excitation. Since volume production rely on H_2 molecules, the plasma with low dissociation degree is preferable. In the volume source two opposite plasma conditions (electron temperature) are required. For this reason, the volume sources are virtually divided into two parts with the help of a magnetic filter field as depicted in Fig. T.1.1.

For long pulse >1000 sec beam operation, volume source is more desirable than surface source, because with the operational time the performance of the surface source would deteriorate due to the surface degradation by the sputtering. A significant improvement in the volume source performance has been observed by adding small amount of cesium (Cs) into the discharge. It has been shown[4] that with the addition of Cs, the process of negative ion formation on the surface dominate in a volume source. This Cs effect gives a big boost to the volume sources. The maximum H^- ion current density from negative ion source so far achieved is from a cesiated H^- ion source and is about 30-100 mA/cm^2.

II. Destruction of H^- ions

The important ways in which the H^- can be lost are:

a. Electronic detachment (ED): The binding energy for the loosely bound electron in an H^- ion is ~ 0.75 eV. If an electron having energy above 0.75 eV collides with an H^- ion, it will destroy it by stripping the loosely bound electron.

$$H^- + e \rightarrow H + 2e$$

The reaction rate of the ED reaction increases with electron temperature. To minimize the ED processes near the extraction grid, the electron temperature near that region should be below 1eV.

b.Mutual neutralization (MN): The neutralization reactions are the most dominant H^- ion loss process.

$$H^- + H^+ \rightarrow 2H$$

$$H^- + H_2^+ \rightarrow H_2 + H$$

$$H^- + H_3^+ \rightarrow 2H_2$$

In spite of this loss mechanism, the space charge compensation principle requires positive ions in the extraction region to extract negative charged particles.

c. Associative detachment (AD): AD reaction and ED are inter-linked and create a cascade effect. To avoid this destruction process, the pressure, the atomic density and the electron temperature in the extraction region should be kept low

$$H^- + H \rightarrow H_2 + e$$

$$H^- + H_2 \rightarrow H + H_2 + e \text{ (stripping loss)}$$

III. Computer Simulation studies for H^- Ion source

RF power requirement of an ion source for a given hydrogen flow rate have been calculated analytically through computer simulations [11] considering the plasma fluid model and using energy and particle balance equations. The total power requirement for the ion source has been computed using energy and particle balance (Fig.T.1.2). Finally various

parameters of the arc discharge and RF discharge have been computed by modelling the plasma generation mechanism through arc and RF discharge [12]. The required plasma density is found to be ~10^{19} m^{-3}.

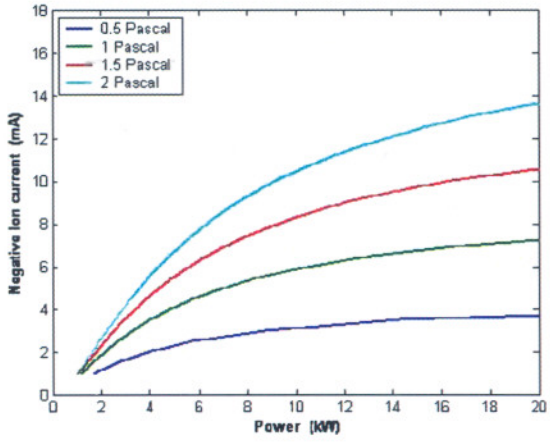

Fig.T.1.2 Variation of RF power absorption in the H⁻ ion source plasma with H⁻ ion current at different gas pressure in the plasma chamber

a. Study of multi-cusp magnetic field in a cylindrical plasma chamber for H⁻ Ion source

Multi-cusp magnetic field configuration has been found to be the most suitable technique for plasma confinement for generation of H⁻ ions through volume production [6-8]. It has the capability to generate uniform and dense plasma that can produce both high and stable negative ion current density in the presence of appropriate filter magnetic field.

We have used the vector potential and Fourier decomposition method to determine the magnetic field intensity variation in the cylindrical chamber which shows a power law radial dependence rather than the exponential form (which has generally been considered by most of the authors as the best approximation). In fact the exponential functional fit has been used with some correcting factors to predict the behaviour of magnetic field in multi-pole arrangement. The expression we have derived for correctly predicting the absolute value of n^{th} harmonic of magnetic field is

$$|B_n| = \frac{N}{R} n a_n \left(\frac{r}{R}\right)^{n \cdot N - 1} \qquad \text{-------(1)}$$

Where 'a_n' is the n^{th} Harmonic coefficient (decided by the magnetization), R is the radius of the chamber and N is pair of magnets. For the same arrangement the conventionally used exponential dependence is

$$|B_n| = \frac{N}{R} n a_n \exp\left(-\frac{n.N.y}{R}\right) \qquad \text{------(2)}$$

Here y is the distance measured from the surface of the plasma chamber. Accurate cusp-magnetic field measurement has been carried out for two sets of permanent magnets to verify above predictions, (12.5mm x 25mm x 50mm; wide magnets and 12.5 mm x12.5 mm x50mm; square magnets) using the Hall-probe method. Fig.T.1.3(a-b) shows two magnetic multi-cusp cylindrical chambers and their field measurement shows that the power law predicts the field free region much more accurately as compared to the exponential dependence. The power law dependence shows excellent agreement with the actual data. The field free region as per equation (1) is nearly three times more as compared to the one estimated using equation (2). The contributions up to two harmonics have been plotted for both equations (1) and (2) (Fig.T.1.3). The results have been reported in an international conference [6].

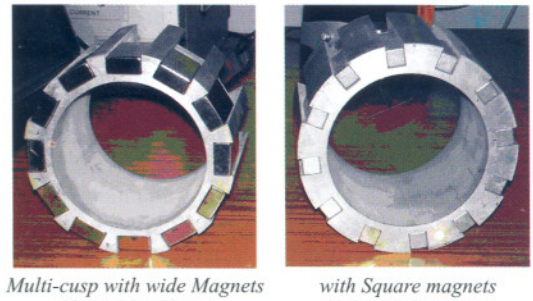

Multi-cusp with wide Magnets 12.5 x 25 x 50 mm

with Square magnets 12.5 x 12.5 x 50 mm

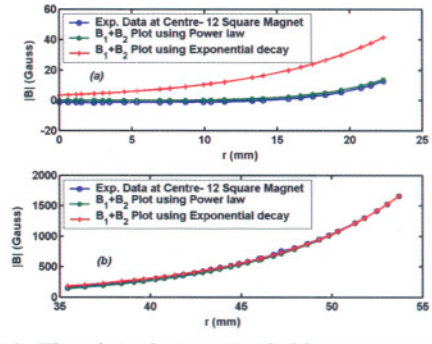

Fig.T.1.3 The plot of magnetic field measurement data (blue curve) compared with exponential form (red curve) and power law form (green curve) for 12 square shape permanent magnets surrounding the plasma chamber. In the central region (a) and near the chamber surface(b). considering the contributions up to two field harmonics

The knowledge of accurate field free region is crucial for H⁻ ion source since (i) the plasma simulation require the knowledge of magnetic field in the central region of plasma chamber (ii) the placement of filament or RF antenna and electron filter magnet and proper design of extraction geometry (iii) the field in the central region affects the cusp loss width, that helps in deciding the power supply requirement and (iv) it is essential for analyzing the results of

plasma diagnostics. However, the use of Permanent Magnet (PM) demands that their temperature and hence the plasma chamber which is in direct contact with it, should not exceed the maximum operating temperature. Although the tolerance limits of Permanent Magnets differs and is around 140°C for NdFeB type magnets, but considering the sensitivity of the plasma confinement on magnetic field and the requirement of greater uninterrupted life of ion source, we have considered the tolerance limit of ~60 °C . Otherwise, permanent magnet performance will be affected and thermal stress can damage their magnetic properties.

b. Cooling arrangement for plasma chamber

With 10% duty factor and ~60 kW peak power dump on the plasma chamber during arc discharge, the effective power dumped is 6 kW(maximum duty factor= 10%) on to the surface area of 0.0452 m^2, which gives heat flux of $1.7x10^5$ W/m^2. We have considered the steady state analysis: hence a uniform distribution of heat flux on the inner walls of the plasma chamber, which behaves like a heat source, can be assumed. ANSYS 10.0 has been used for modelling and analysis [13]. Three kind of cooling channels, Cylindrical single hole channel (8 mm diameter adjacent to each bar magnets, Rectangular (260 mm x 2 mm) and Multi-channel (3mm diameter, 5 channels) underneath the bar magnets (shown in Fig.T.1.4) have been considered. The cooling is to be done by turbulent flow of chilled water at 7°C apart from cooling of outer surface by air at room temperature (27°C). The important parameters are water flow velocity, Hydraulic Diameter, Reynolds number, Nusselt Number and convective heat transfer coefficient.

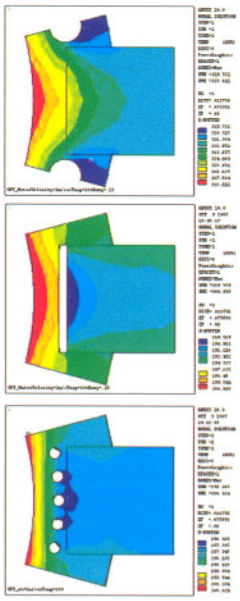

Fig.T.1.4 For OFHC Cu chamber

Heat removal calculations were carried out for the OFHC copper and SS plasma chamber so as to protect the 12 PM's placed around the chamber along its length. Water flow rate for various coolant channels in Cu and SS plasma chamber have also been calculated [13]. The difference in maximum and minimum temperature for OFHC Cu chamber is ~ 10°C whereas for SS it is ~45°C. Typical results obtained for OFHC Cu are shown in the table below.

Table T.1.1 Value of Maximum and Minimum Temperature and flow rates obtained through FEA modelling for OFHC Cu.

	Water Velocity m/sec	Water Flow rate Lit/min	OFHC Cu (Ku = 393 $Wm^{-1}K^{-1}$)	
			Max. Temp (K)	Min. Temp .(K)
Rectangular	0.5	18.72	312	300
Channels	1	37.44	300	290
Multi Hole	0.5	12.72	314	309
Channels	1	25.44	301	296
Single Hole	0.5	18.06	358	349
Channels	1	36.19	329	319

Even though the volume occupied by the five multi channels (4241mm^3) is less than rectangular channel (6240mm^3) or single channel (6032mm^3) but the cooling achieved is comparable to that of rectangular channel and much better than single channel, for same flow velocity. It seems that the arrangements for rectangular channels may be difficult to machine and fabricate, as flowing water should not come in contact with permanent magnets.

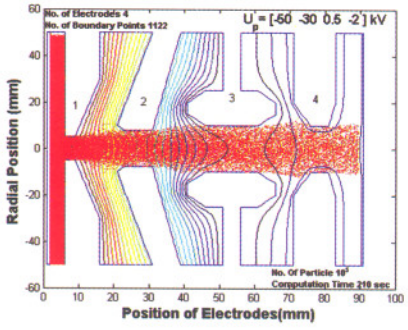

Fig.T.1.5 The extraction of negative ions, through tetrode geometry is shown. The red dot represents the H ions and the electrodes numbered as 1, 2, 3and 4 represents plasma, extractor, accelerator and screening electrode respectively. The electrode shapes and equipotential lines are shown taking into account the space charge effect. A total of 10^5 particles have been tracked in the PIC code and it took about 210 secs, to reach a convergent solution

The PIC simulation code has been developed which incorporates elementary module of the Monte Carlo code algorithm. The extraction code is functioning and has been tested for H^- ions. A Fast Fourier Transform (FFT) based Poisson solver has been used coupled with capacitance matrix to incorporate the arbitrary electrode geometry. In order to overcome the limitations of FFT solver, a matrix decomposition based Poisson solver has been developed (see Fig.T.1.5).

c. Filter magnet design study for H^- ion source

Magnetic filter plays an important role in allowing formation of H^- ions near the extraction region as well as reduce their destruction probability. It is generally employed near the extraction grid, transverse to the chamber axis. This effectively splits the plasma chamber of the ion source into two regions as already shown in Fig.T.1.1. The hot or driver region, where vibrationally excited H_2 molecules are formed and the extraction region where low energy electron attached itself to the vibrationally excited molecules through dissociative attachment process and generate H^- ions which are extracted using suitable extraction geometry. The filter field obstructs the flow of hot electrons and allows only low energy electrons to drift through the driver to extractor region. There are few crucial parameter associated with the design of the magnetic filter field. The strength of the dipole magnetic field should be strong enough to magnetize the electrons but weak enough to practically have no effect on the charged ion species like H^+,H_2^+,H_3^+ or H^-. The filter field is applied near the extraction region hence it should not influence the extraction of negative ion beam. For this the filter field must decay rapidly along the chamber axis in the extraction region. It should not alter the cusp magnetic field configuration employed for the confinement of the plasma inside the driver region and hence must have limited spatial extent and applied in the field free region [5] of the cusp geometry. Moreover, it should not affect the uniformity of the plasma near the extraction region or else it will alter the desired beam quality substantially. The fringing field associated with the filter magnets can affect the emittance of the H^- ion beam. It can lead to substantial loss of the negative ion beam. Thus, in order to optimize such effect one needs to carefully design the filter field. Some of the essential features of the filter field in combination with the electron steering magnet can be understood using magnet model which replaces it with equivalent magnetic charges +q at north pole and −q at south pole. Fig.T.1.6 shows the schematic of filter magnets and electron steering magnets. Replacing the permanent magnets with magnetic charge separated by effective distance l_1 and l_2 one can compute the magnetic field on the symmetry axis (z axis).

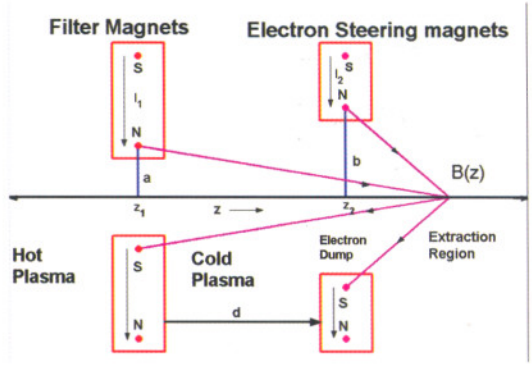

Fig.T.1.6 Schematic model of filter magnets and electron steering magnets

An appropriate functional form for the variation of the filter field along the chamber axis is:

$$B(z) = \frac{ka}{\left[a^2 + (z - z_1)^2\right]^{3/2}}$$

where $k = B(z_1)\, a^2$ and 2a is the pole gap and z_1 is the coordinate where |B| is maximum.

The electron and negative ion separation

We compute the magnetic field required to deflect the electron by 90^0, using the dipole of length 2 cm, one get B≈ 310Gauss. For non-relativistic case and small angle deflection, the above relation for deflection angle θ reduces

$$\theta = \frac{qdB}{\sqrt{2m\kappa_e}}$$

The electron and H^- ions coming out of ion source will see same sheath potential and hence both of them will get accelerated by same kinetic energy. Thus if θ_e and θ_p is the deflection angle of electron and H^- ions then the ratio of their angular deflection is inversely proportional to their mass i.e

$$\frac{\theta_e}{\theta_p} = \sqrt{\frac{m_p}{m_e}} \approx 43$$

i.e. the electrons will be deflected 43 times more than H^- ion in the same field. To deflect electron by 90^0 the H^- ions will be deflected approximately by 2^0. To correct this small deflection of the trajectory of H^- ions the ion source is itself tilted by this amount in opposite direction.

d. Filter and steering magnetic field measurements

The pole gap for filter magnet (a) is 2.5cm and for steering magnet (b) it is 3.5cm. The large gap at the steering magnet is also desirable for flexibility in the design of extraction geometry, which is currently under way. Then the distance between the filter magnet and steering magnet is varied and magnetic field profile is measured. Fig.T.1.7 shows the plot of combined magnetic field of filter magnet and electron steering magnet. The result obtained by FEM model has also been plotted along with it. It shows that minimum separation between the two should be 6 cm, if it is decreased further then the overlap between the two will be more than 100 Gauss [14]. This field, at extraction aperture where meniscus is formed and bias colours are located, can affect the extraction of H^- ions and the properties of the extracted ion current like divergence, emittance, and energy spread etc. To reduce the gap, the filter field must decrease more rapidly than what one get. This can be achieved if fringing field is reduced. An interesting way to do this is to wrap iron or new metal around the filter magnet leaving the pole face. This will reduce the fringing field considerably by providing easy alternative path to the fringing magnetic field lines. Preliminary investigation carried out in this direction shows good result. Further suitable pole shape of permanent magnets may also be able to achieve this.

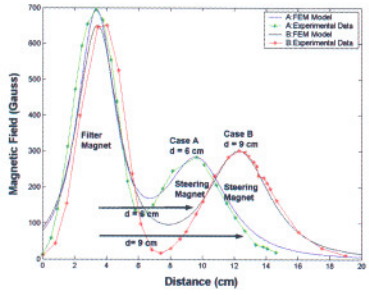

Fig.T.1. 7 Experimental results and corresponding FEM results

IV. Simulation of H^- ion extraction

The design of a high current H^- ion source can utilize both volume and surface production processes. A controlled Cs insertion helps in enhancing the H^- ion current. Simulation results for H^- ion extraction are presented, from plasma region to RFQ entrance using the software nIGUN[15], which consider the role of sheath formation in the plasma chamber near the chamber wall close to the extraction aperture. Presence of various ion species like H^+,H_2^+,H_3^+, H^-,e and Cs^+ etc. have been considered for modelling of sheath and effect of space charge in the extraction region. Further, it has been shown that proper biasing of plasma electrode in the non-Cesiated ion source helps in building up the vibrationally excited H_2 molecules resulting in higher H^- ion extraction. Finally different negative ion extraction geometries studied using the nIGUN code calculations to optimize the ion beam properties for the cesiated and non-cesiated ion sources are discussed [16].

a. nIGUN-2D simulation

The program nIGUN utilizes a new theory of multi-particle plasma sheath for H^- ion extraction [15] which has been used to modify the ion extraction program [16]. The stability of convergence is obtained for the nonlinear sheath region by directly inserting the analytical space charge according to the Poisson equation for each mesh point above the wall potential. The field strength in the extraction gap is used to determine the densities of all the species by the program. nIGUN has built in boundary processing to define internal electrodes and Neumann and dielectric boundaries. Close to extraction region the positive ions, protons and Cs ions from the plasma source are reflected by the extraction field resulting in a creation of virtual cathode. It is assumed in the program that the space charge of H^- ions counteracts the extraction field without creating a saddle point of potentials.

b. Cesiated H^- ion source

In order to simulate the cesiated ion source with suitable low energy beam transport (LEBT) structure to match with the input of a radio frequency quadrupole (RFQ) including the electrostatic chopping of the beam, we consider typical geometry used for SNS source as shown in Fig.T.1.8

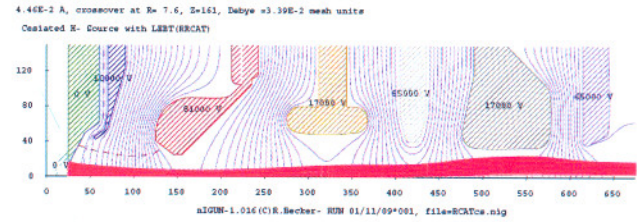

Fig.T.1.8 Simulation of Cesiated H^- ion source with LEBT structure from plasma to RFQ entrance

c. Non-Cesiated H^- Ion Source:

With the success of DESY H^- ion source [10] operating without Cs insertion in the plasma chamber having stable ion current and longer lifetime, employing RF antenna to generate the plasma and create the arc discharge, we have performed the simulation of such source using simple extraction geometry of two electrodes. The main difference in this source configuration is the biasing of the plasma electrode which is free from cesium. The negative bias of -15 V is used on the

plasma electrode or cylindrical collar attached with it that helps in acceleration of protons from the main plasma region enabling them to create more efficiently highly vibrationally excited hydrogen molecules to further enhance the H^- ion formation through volume production mechanism in the vicinity of extraction region. In order to simulate such ion source we begin with initial parameters to satisfy the proper conditions for inverted sheath formation near the extraction region and ensure that there is no virtual cathode appearance due to improper selection of initial particle parameters.

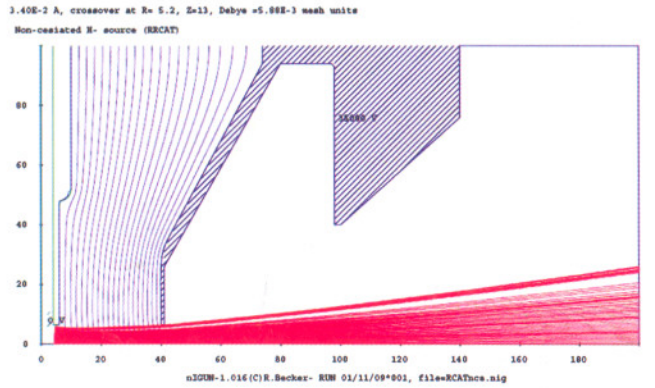

Fig.T.1.9 Simulation of non-cesiated ion source with diode extraction system.

The H^- ion current of 34 mA is extracted from the diode geometry as shown in Fig.T.1.9; however the emittance value of 0.59π mm mrad is obtained [17]. Further, it is noticed that there is no loss of ions due to puller electrode which has same aperture as plasma electrode.

V. Conclusion

Development of H^- ion source has been initiated. Attempts have been made to study the characteristic design of H^- ion source using computer simulations. Various processes of H^- ions formation and destruction have been incorporated in it. Hybrid scheme utilizing volume and surface production of H^- ions will be adopted in the design of H^- ion source. One of the common features of most of such sources has been to make a multi-cusp magnetic field design to confine the plasma in the cylindrical plasma chamber in the field free region. This aspect has been studies through FEM analysis followed with experimental measurements of magnetic field that shows excellent agreement. We have derived power law functional form of magnetic field dependence inside the cylindrical plasma chamber which can be very useful in accurate analysis and study of H^- ion plasmas.

Further, the cooling arrangement for the plasma chamber has been worked out through FEM simulations which can protect the permanent magnets from thermal effects and maintain the lower temperature adjacent to permanent magnets in contact with the plasma chamber inner wall. The filter field studies were carried out to optimize the placement of dipole filter magnet between cusp magnetic field and steering magnets for rejection of electrons from extraction region. The extraction geometry for 2, 3, 4 and 5 electrodes has been designed with the help of nIGUN code for both, with and without Cs insertion in the plasma chamber. Based on above work and some further studies, first prototype H^- ion source will be designed and tested.

References:

1. G.I. Dimov, Rev. Sci. Inst. 67, 3393-3404 (1996).
2. www.iter.org
3. Yu.I. Belhenko et al., Nucl. Fusion 14, 113 (1974).
4. M. Bacal et al., Phys. Rev. Lett. 42, 1538 (1977).
5. Ajeet Kumar, V.K. Senecha and R.M. Vadjikar, Ist Int. Nat. Conf. Neg. Ions, Beams and Sources, France, AIP Conf. Proceed. Vol. 1097, 137-148 (2008).
6. H. Oguri et al., Phys. Rev. Special Topics-Accel. & Beams 12, 010401 (2009).
7. J. Peter, Rev. Sci. Inst. 79, 02A515 (2008).
8. R.F. Welton et al., Proceed. PAC-07, FROAAB02, 3774 (2007).
9. M.Bacal, Nucl. Fusion 46, S250-S259 (2006)
10. M.Bacal,A.Hatayama and J. Peter, IEEE Trans. On Plasma Sciences 33, 1845-1871 (2005).
11. Ajeet Kumar,V. K. Senecha and S. Kotaiah, Indian Particle Accelerator Conference, InPAC-06, E02, 227 (2006).
12. Ajeet Kumar,V. K. Senecha and S. Kotaiah, Asian Particle Accelerator Conference, APAC-07, TUPMA115,RRCAT, Indore (2007).
13. Ajeet Kumar, V.K. Senecha and S.Kotaiah, Proceed. of DAE-BRNS-PSI Symposium on Ion Beam Technology and Applications(SIBTA-07) Page 261-269; Edited by: P.Roychowdhury and D.S. Patil; BARC, Mumbai, 19-21 Sept. (2007).
14. Ajeet Kumar, V.K. Senecha, Indian Part. Accel. Conf. (InPAC09), MDT-05, RRCAT, Indore (2009).
15. R. Becker, Rev. Sci. Inst. 75, 1687 (2004).
16. R. Becker, Rev. Sci. Inst. 77, 03A504 (2006).
17. V.K. Senecha,R.M. Vadjikar, Ajeet Kumar, Indian Part. Accel. Conf. (InPAC09), EIS-03, RRCAT, Indore (2009).